GLOBAL HORIZONTAL IRRADIANCE ESTIMATION IN TROPICAL TERRAIN USING SEMI-EMPIRICAL APPROACH: A SEASONAL ASSESSMENT IN WEST JAVA, INDONESIA.

Pranda Mulya Putra Garniwa[1], Rifdah Octavi Azzahra[2], Muhammad Dimyati[1]

[1]Department of Geography, Faculty of Mathematics and Natural Science, University of Indonesia

e-mail: pranda.mg@ui.ac.id

Received: 24-05-2025; Revised: 08-06-2025; Approved: 13-07-2025

Abstract. Accurate estimation of solar irradiance is essential for optimizing solar energy planning, particularly in tropical regions like Indonesia, where observational infrastructure is limited and atmospheric conditions are highly variable. This study addresses the challenge by applying the Perez semi-empirical model to estimate Global Horizontal Irradiance (GHI) across West Java, a topographically diverse province with seasonal weather dynamics. The model integrates satellite-based reflectance data from the GK2A satellite and atmospheric parameters from AERONET, using a spatial resolution of 0.5 km. GHI estimation was conducted for four tropical seasonal phases: the rainy season, transition to dry, dry season, and transition to rainy. Model validation was performed using hourly GHI measurements from two BMKG stations in Indramayu. The Perez model showed strong performance, with RMSE ranging from 146.96 to 163.52 W/m² and relative RMSE below 38%. The results indicate that the model reliably captures both seasonal and spatial variations of solar radiation under tropical atmospheric conditions. Spatial analysis reveals a consistent pattern: lowland and coastal areas receive significantly higher GHI compared to highland regions, which are affected by cloud formation and orographic effects. These findings confirm the model's suitability for tropical solar forecasting and offer valuable insights for identifying high-potential zones for photovoltaic development.

Keywords: *Solar Irradiance, Semi-empirical, Topography, Estimation, Tropical Region*

1 INTRODUCTION

Global energy demand continues to surge, driven by population growth and widespread electrification. The International Energy Agency (IEA) projects a 45% increase in global energy demand by 2030, with the electricity sector contributing significantly to this growth (IEA 2023; Economist Intelligence Unit 2023). In Indonesia, the population is expected to grow from 284.086 million in 2024 to 324.05 million by 2045 (Worldometers 2024), intensifying energy needs, particularly in transportation and industry, which comprised 41% and 39% of electricity consumption in 2019, respectively (Institute for Essential Services Reform 2021). Per capita electricity use rose from 1,173 kWh in 2022 to 1,337 kWh in 2023—a 13.98% increase (ESDM 2024). West Java is the country's largest electricity-consuming province, distributing 56,226.11 GWh in 2022, with an additional 4.12% rise in 2023 (PLN 2024). These trends highlight the urgent need for sustainable alternatives. Among them, solar energy emerges as a promising solution, especially for tropical regions like Indonesia, offering reliability and abundance to support future energy transitions and reduce dependence on fossil fuels.

Despite global decarbonization efforts, Indonesia's energy mix remains heavily reliant on fossil fuels—coal contributed

42.38% and oil 31.40% of the primary energy supply in 2023 (ESDM 2023). Coal-fired power plants alone are responsible for about 66% of national CO_2 emissions (IEA 2024). Simultaneously, domestic reserves are declining; proven oil reserves dropped nearly 50% between 2018 and 2019, with projections indicating potential depletion within two decades if no new discoveries occur (ESDM 2019; ESDM 2021). These developments underscore the urgent need to accelerate a transition toward renewable energy, with solar energy positioned as a critical component of Indonesia's sustainable energy strategy.

Solar technologies—such as photovoltaics and concentrated solar power—are integral to achieving carbon neutrality (Maka et al. 2024). However, the intermittency of solar irradiance introduces operational uncertainties, highlighting the need for accurate solar resource assessment (Albadi and Al-Badi 2021). While ground-based measurements are highly accurate, their spatial coverage is limited by cost and technical constraints (Halabi et al. 2018). Consequently, models integrating satellite imagery and meteorological inputs have become essential tools for estimation (Escobar et al. 2014). Among various approaches—physical, empirical, semi-empirical, and machine learning (Kleissl 2013)—semi-empirical models like Perez's provide a pragmatic balance between complexity and data availability, making them especially useful in data-sparse regions such as Indonesia (Perez et al. 2002; Scarpa et al. 2018).

Semi-empirical models have shown promising performance even under diverse sky conditions. For example, (Chen *et al.* 2022) demonstrated that semi-empirical satellite-based models could achieve normalized RMSE values around 20–23% for GHI estimation. Although machine learning models, including deep learning frameworks, have emerged as powerful tools for irradiance estimation (Gürel *et al.* 2023), their reliance on large, high-quality datasets and significant computational capacity can be prohibitive in many developing regions (El-Amarty *et al.* 2023). Semi-empirical models, therefore, remain highly relevant for practical applications, especially for initial solar resource assessments.

Beyond the estimation of solar irradiance, the spatial variability of solar resources presents another layer of complexity that is especially critical for geographical studies. Solar irradiance is not uniformly distributed over a region; it is strongly influenced by topographical features such as elevation, slope, and aspect (Zhang *et al.* 2022). Higher altitudes may experience different solar exposure patterns compared to low-lying areas due to variations in atmospheric thickness, cloud cover frequency, and terrain shading effects (Alpandino 2011). In regions with complex topography like West Java, these spatial factors play a pivotal role in determining the true solar resource potential.

Several studies have highlighted that accurate solar resource mapping must consider the spatial heterogeneity introduced by geographical factors (Cai *et al.* 2024; Zhang *et al.* 2024; Sarr *et al.* 2011). Topography can alter the angle of incidence of solar radiation, cause orographic cloud formation, and influence local microclimates, thereby affecting both the magnitude and variability of surface-level solar irradiance (Napoli *et al.* 2019). Geospatial analysis methods, often using digital elevation models (DEMs), remote sensing imagery, and spatial interpolation techniques, are widely applied to characterize these variations and produce detailed solar potential maps (Zhang *et al.* 2022).

In this context, understanding the spatial distribution of GHI is essential not only for estimating total energy yields but also for guiding site selection for photovoltaic installations, informing land-use planning, and optimizing regional energy development strategies. Hence, solar resource assessment cannot be decoupled from spatial analysis, particularly in geographically diverse settings.

Based on this understanding, the present study is designed with a twofold objective. First, to estimate Global Horizontal Irradiance (GHI) across West Java using the Perez semi-empirical model, leveraging available meteorological inputs. Second, to

evaluate the spatial distribution patterns of the estimated GHI with a particular focus on analyzing how topographical features, especially elevation, influence solar radiation availability across the region. By bridging solar resource estimation with geographical spatial analysis, this study aims to contribute both to the field of renewable energy development and to the growing body of work at the intersection of physical geography and energy studies. The findings from this research are expected to inform solar energy planning efforts in Indonesia by providing more geographically detailed insights into solar resource availability, and to support the broader national agenda of transitioning towards a more sustainable and low-carbon energy future.

2 MATERIALS AND METHODOLOGY

2.1 Study Area

This study was conducted in West Java Province, located in the western part of Java Island, Indonesia. Covering approximately 3.7 million hectares, the province lies between 104°48′–108°48′ E and 5°50′–7°50′ S, bordered by Jakarta and Banten to the west, Central Java to the east, the Java Sea to the north, and the Indian Ocean to the south. It comprises 18 regencies and 9 cities, encompassing a range of landscapes from coastal plains to volcanic highlands, making it one of Indonesia's most geographically and demographically diverse provinces.

Topographically, West Java is divided between northern lowlands and central–southern highlands, with elevations exceeding 2,000 meters above sea level (BPS 2023). This variation influences cloud formation, atmospheric humidity, and solar irradiance patterns, making the region ideal for studying the spatial variability of solar radiation (Tscholl *et al.* 2022). The province lies within the tropical monsoon zone, characterized by distinct wet and dry seasons and annual rainfall ranging from 2,000 to 4,000 mm (BNPB 2022). According to the Köppen–Geiger classification (figure 2-1), the province exhibits five climate types—Af, Am, Aw, Cfb, and Cwb—primarily driven by elevation and proximity to the sea (Beck *et al.* 2023).

Model validation was conducted using data from the Indramayu meteorological station, located in the flat northern coastal plain. This lowland site provides high-quality ground-based irradiance data and serves as a reliable reference for evaluating the Perez model's performance in tropical low-elevation environments.

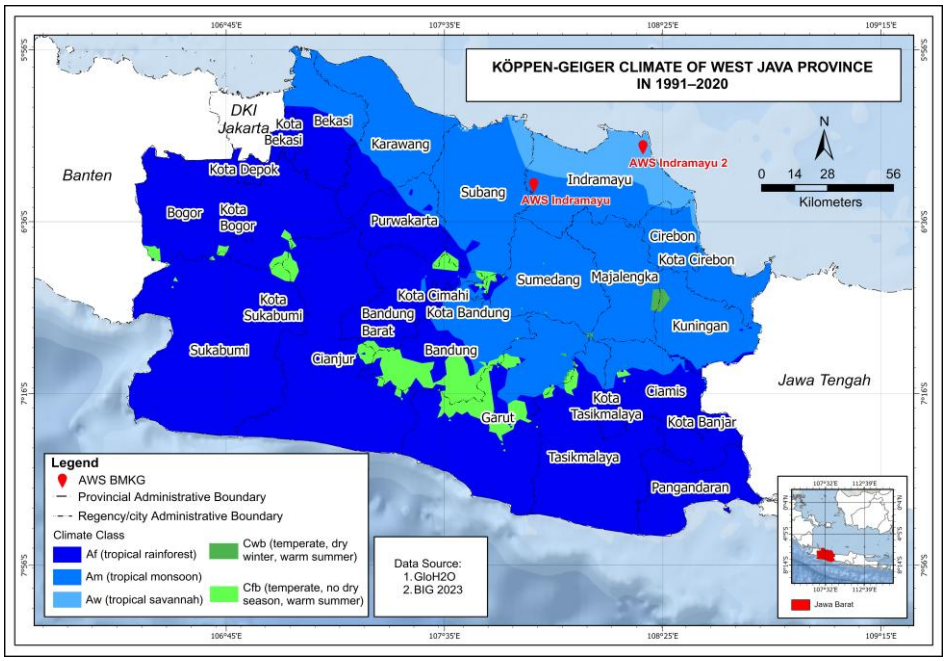

Figure 2-1: Köppen-Geiger Climate Classification of West Java Province (1991–2020).

2.2 Data and Sources

This study utilized both primary and secondary datasets to estimate and validate solar irradiance across West Java, as shown in Table 2-1. Primary data were obtained from the Aerosol Robotic Network (AERONET), including hourly measurements of Global Horizontal Irradiance (GHI), Aerosol Optical Depth (AOD), Angstrom turbidity, water vapor, and satellite zenith angle. These parameters, recorded using standardized radiometric instruments at AERONET sites in Jakarta and Bandung, served as critical inputs for model validation and atmospheric correction. However, the spatial coverage of AERONET in West Java is limited, with stations primarily located in northern lowland areas. This limits the representativeness of the validation results, particularly for mid- and high-elevation zones that exhibit more complex terrain and microclimatic variability.

Secondary data sources included satellite-derived cloud information and topographic datasets. Reflectance values from the visible channel of the GEO-KOMPSAT-2A (GK2A) satellite, provided by the Korea Meteorological Administration (KMA), were used to estimate cloud indices required by the Perez model (Perez et al. 2002). These satellite data offer hourly temporal resolution and a spatial resolution of 0.5 × 0.5 km, enabling localized characterization of sky conditions. While satellite-based reflectance retrievals can be subject to geometric distortions, especially over heterogeneous land surfaces or steep terrain, the Perez model includes correction mechanisms for solar elevation, backscattering, and air mass to reduce such effects. Additionally, cloud contamination is

systematically addressed through the Cloud Index (CI), a dynamic variable derived from reflectance values and used to scale clear-sky irradiance to account for cloud coverage. This enables the

Table 2-1: Primary and Secondary Data, Measurement Methods, and Sources.

Type	Data	Acquisition
Primary	Aerosol Optical Depth (AOD)	Ground-based measurements of AERONET
Primary	Water Vapor	Ground-based measurements of AERONET
Primary	Ångström Turbidity	Computed from spectral wavelength data
Primary	GHI	Direct measurement using pyranometer and weather station at hourly intervals (BMKG)
Primary	Solar Zenith Angle/Sun Elevation Angle	Computational calculation based on recording station location and solar position relative to zenith
Primary	Backscatter Angle	Computational calculation of the direction of incoming solar radiation relative to Earth's position
Primary	Air Mass	Computational calculation of atmospheric thickness traversed by solar radiation
Secondary	GK2A Satellite Image Reflectance	Satellite data covering Java Island with hourly intervals.
Secondary	Site Elevation	Digital Elevation Model (DEM), processed for elevation and slope
Secondary	Satellite Zenith Angle	GK2A satellite zenith angle data

model to dynamically capture spatiotemporal variations in atmospheric transparency.

Data processing and model implementation were conducted using Python (NumPy, Pandas, Rasterio) and QGIS for spatial analysis, overlay, and visualization. Microsoft Excel supported preliminary data handling and statistical summarization. This integrated approach—merging satellite observation, ground validation, and spatial-topographic analysis—ensures methodological robustness and enhances the accuracy of irradiance estimation under diverse tropical conditions.

2.3 Estimation Method: Perez Semi-Empirical Model

Prior to implementing the Perez model, a quality control (QC) procedure was applied to ensure that input data met the required standards for accuracy and temporal consistency. The QC criteria are summarized in Table 2.2, which outlines filtering rules designed to exclude erroneous or physically implausible observations. These include solar zenith angles greater than 85°, negative values for GHI, DNI, and DHI, and constraints on the DHI/GHI ratio based on zenith angle and irradiance thresholds. These filters were used to eliminate nighttime values and low-angle sun conditions that typically introduce high uncertainty in irradiance modeling.

The dataset, covering January to December 2022, was also interpolated using a linear technique to fill temporal gaps. This step, implemented in Python using the Spyder environment, assumed gradual transitions between known values and restored continuity in cases of missing data. Standardization to an hourly time step was enforced to match the temporal resolution of satellite-based inputs. By combining value filtering, temporal resampling, and interpolation, the QC process enhanced the reliability of atmospheric and irradiance inputs. This preprocessing step ensured that all subsequent modeling and validation efforts were based on a consistent and high-quality dataset.

Tabel 2-2: Quality Control (QC) criteria applied to solar irradiance datasets.

Parameter	Criterion
Sun zenith angle (θ_z)	< 85°
GHI, DNI, DHI	> 0 W/m²
DHI/GHI	< 1,05 for θ_z < 75° and GHI > 50 W/m²
DHI/GHI	< 1,10 for $\theta_z \geq 75°$ and GHI > 50 W/m²

The Perez semi-empirical model was applied in a five-stage workflow to estimate surface-level Global Horizontal Irradiance (GHI) across West Java. These stages included: (1) pixel-level satellite reflectance correction, (2) cloud index (CI) estimation, (3) Linke Turbidity (TL) calculation, (4) clear-sky irradiance (GHIC) computation, and (5) the final GHI estimation under all-sky conditions.

In the first stage, pixel reflectance values were extracted at hourly intervals from GK2A satellite imagery, capturing top-of-atmosphere conditions. Reflectance was sampled over West Java throughout 2022. To reduce optical and geometric distortion—primarily caused by air mass (AM) and backscattering—pixel normalization was applied. The Perez model applies corrections based on solar elevation angle (γ), AM, and long-term satellite reflectance characteristics. The normalization factor (CC_P) was calculated following Garniwa *et al.* (2021) and expressed as a function of AM, elevation, and solar geometry parameters [Eq. 1].

$$CC_P = \frac{C_{sat} AM \varepsilon}{2.283\gamma^{-0.26}\exp(0.004\gamma)} \quad (1)$$

Following normalization, the Cloud Index (CI) was derived to quantify cloud cover based on the difference between observed and reference reflectance values. Using the formulation adapted from Beyer *et al.* (1996) and Hammer *et al.* (2003), CI was computed as a ratio between the normalized pixel reflectance and its theoretical minimum and maximum limits [Eq. 2]. CI values range from 0 (clear sky) to 1 (overcast), and

serve as a core input to the Perez model for cloudiness representation.

$$CI = \frac{CC - C_{min}}{C_{max} - C_{min}} \quad (2)$$

In the third stage, Linke Turbidity (TL) was calculated to represent atmospheric attenuation caused by aerosols and water vapor. TL is critical for adjusting clear-sky irradiance under local atmospheric conditions. The Ångström turbidity coefficient (β) was first derived from AOD and wavelength data [Eq. 3]. TL was then computed using Remund *et al.* (2003) formulation, which integrates β with water vapor concentration (w) obtained from AERONET measurements [Eq. 4].

$$\beta = \frac{\tau_{a,\lambda}}{\lambda^{a}} \quad (3)$$

$$TL = (1.8498 + 0.2425w - 0.0203w^2) + (15.427 + 0.3153w - 0.0254w^2)\beta \quad (4)$$

The fourth stage involved the estimation of clear-sky irradiance (GHIC), which represents the theoretical solar radiation received under cloud-free conditions. GHIC was calculated using a modified radiative transfer expression incorporating TL, AM, and site elevation. The formulation includes empirical correction terms for Rayleigh scattering and aerosol absorption, adjusted by altitude-dependent coefficients [Eq. 5–9]. This value forms the baseline for all-sky GHI estimation in the Perez model.

$$GHIC = cg1 I_0 \cos\theta_z exp[-cg2AM(fh1 + fh2(TL - 1))] exp(0.01AM^{1.8}) \quad (5)$$

$$fh1 = exp\left(\frac{-z}{8000}\right) \quad (6)$$

$$fh2 = exp\left(\frac{-z}{1250}\right) \quad (7)$$

$$cg1 = 0.0000509z + 0.868 \quad (8)$$

$$cg2 = 0.0000392z + 0.0387 \quad (9)$$

In the final stage, GHI was computed by scaling GHIC with a clear-sky index (k_c), which translates CI into a transmission factor. For the Perez model, (k_c) is expressed as a fifth-order polynomial function of CI [Eq. 10]. The resulting GHI is calculated as a product of GHIC and this correction factor [Eq. 11]. This step integrates atmospheric and cloud-related effects, producing the final GHI estimates used for spatial mapping and model validation.

$$k_c = 2.36CI^5 - 6.2CI^4 + 6.22CI^3 - 2.63CI^2 - 0.58CI^2 - 0.58CI + 1 \quad (10)$$

$$GHI = k_c GHIC(0.0001 k_c GHIC + 0.9) \quad (11)$$

2.3 Spatial Overlay and Elevation-Based Analysis

To assess how elevation influences the spatial distribution of solar irradiance, a topographic overlay analysis was conducted by integrating the Perez-modeled GHI outputs with a Digital Elevation Model (DEM) of West Java. Using ArcGIS Pro, the GHI estimates—generated at 0.5 × 0.5 km resolution from GK2A imagery—were spatially intersected with elevation data to classify irradiance values across distinct topographic zones.

The study area was divided into three elevation classes: lowlands (0–500 m), mid-elevation zones (500–1000 m), and highlands (>1000 m). For each class, seasonal average irradiance values were computed to evaluate terrain-induced variation under different atmospheric conditions.

The analysis revealed a clear spatial gradient: lowland areas consistently received higher solar irradiance, likely due to thinner atmospheric layers and reduced cloud formation. In contrast, highland zones often exhibited lower irradiance, which may result from orographic cloud development, topographic shading, and localized microclimates. By linking elevation to irradiance patterns, this analysis offers critical insights into how terrain modifies solar resource availability and highlights areas of opportunity or limitation for photovoltaic deployment in complex tropical landscapes.

The use of hourly temporal resolution in this study reflects both methodological considerations and

practical constraints. Hourly data aligns with the observation frequency of the GEO-KOMPSAT-2A satellite and the BMKG ground-based validation datasets, ensuring temporal consistency between modeled and observed values. While sub-hourly data (e.g., 5–15-minute intervals) could potentially capture finer-scale fluctuations in irradiance—important for operational PV system control and short-term forecasting—such data are rarely available across large regions in developing countries. Conversely, daily averages may oversmooth variability, underestimating peaks and ramps that are relevant for system sizing and grid integration. Hence, hourly intervals offer a suitable compromise for estimating GHI at regional scales while maintaining adequate accuracy for pre-feasibility assessments and spatial planning of solar energy infrastructure.

2.4 Metric Accuracy

To evaluate the performance of the Perez semi-empirical model, estimated GHI values were validated against ground-based measurements from the BMKG station in Indramayu. The comparison assessed how well the model captures real-world atmospheric conditions based on statistical error metrics. Four accuracy metrics were used: Root Mean Square Error (RMSE), Relative RMSE (rRMSE), Mean Bias Error (MBE), and Relative MBE (rMBE). RMSE and rRMSE measure the magnitude of prediction errors, while MBE and rMBE indicate the direction of bias—whether the model overestimates or underestimates GHI. Lower values across these metrics indicate better model performance.

$$\mathrm{RMSE} = \sqrt{\frac{1}{n}\sum_{i=1}^{n}(\mathrm{GHI}_{\mathrm{model}} - \mathrm{GHI}_{\mathrm{measurement}})^2} \quad (12)$$

$$\mathrm{rRMSE} = \frac{\sqrt{\frac{1}{n}\sum_{i=1}^{n}(\mathrm{GHI}_{\mathrm{model}} - \mathrm{GHI}_{\mathrm{measurement}})^2}}{\frac{1}{n}\sum_{i=1}^{n}\mathrm{GHI}_{measurement}} \times 100 \quad (13)$$

$$\mathrm{MBE} = \frac{1}{n}\sum_{i=1}^{n}(\mathrm{GHI}_{\mathrm{model}} - \mathrm{GHI}_{\mathrm{measurement}}) \quad (14)$$

$$\mathrm{rMBE} = \frac{\frac{1}{n}\sum_{i=1}^{n}(\mathrm{GHI}_{\mathrm{model}} - \mathrm{GHI}_{\mathrm{measurement}})}{\frac{1}{n}\sum_{i=1}^{n}\mathrm{GHI}_{\mathrm{measurement}}} \times 100 \quad (15)$$

3 RESULTS AND DISCUSSION

3.1 Annual Accuracy

West Java's diverse geography, spanning from low-lying coastal plains to elevated interior highlands, presents a complex setting for modeling solar irradiance. Local factors such as atmospheric moisture, convective cloud dynamics, and terrain-driven shading contribute to spatial variability in solar energy reaching the surface. Despite these complexities, some regions—particularly in the flat northern lowlands—offer more stable atmospheric conditions. This makes them suitable for validating solar irradiance estimation models under relatively uniform surface and climatic characteristics.

Table 3-1: Annual Accuracy of Solar Irradiance.

This study focuses on two observation sites in Indramayu Regency: Indramayu 1 (IDM1) and Indramayu 2 (IDM2). Both are located in northern West Java's coastal lowlands, characterized by minimal terrain variation and relatively consistent daily weather cycles. These physical and atmospheric attributes create favorable conditions for applying semi-empirical models, particularly those sensitive to surface geometry and cloud conditions derived from satellite imagery. Their location provides a robust testbed for evaluating the performance of the Perez model in a tropical lowland setting.

The Perez model demonstrated strong estimation accuracy at both Indramayu sites, as shown in Table 3-1. RMSE was recorded at 163.52 W/m² for IDM1 and 146.96 W/m² for IDM2, indicating a close fit between modeled and observed irradiance values. rRMSE values were also low, with IDM1 at 37.22% and IDM2 at 35.36%. These results suggest that the Perez model was effective in reproducing hourly and daily GHI patterns in this lowland coastal region with relatively low variability and uncertainty. In terms of MBE and rMBE, IDM2 exhibited a small positive bias, with a MBE of +12.57 W/m², indicating a minor overestimation. In contrast, IDM1 recorded a slightly negative bias (MBE of –5.48 W/m²), showing a

tendency to slightly underestimate irradiance. These biases, reflected in the rMBE values of 3.02% and –1.24%, respectively, remain within acceptable operational margins and demonstrate the model's ability to maintain balance in its estimations without strong overfitting or underfitting tendencies.

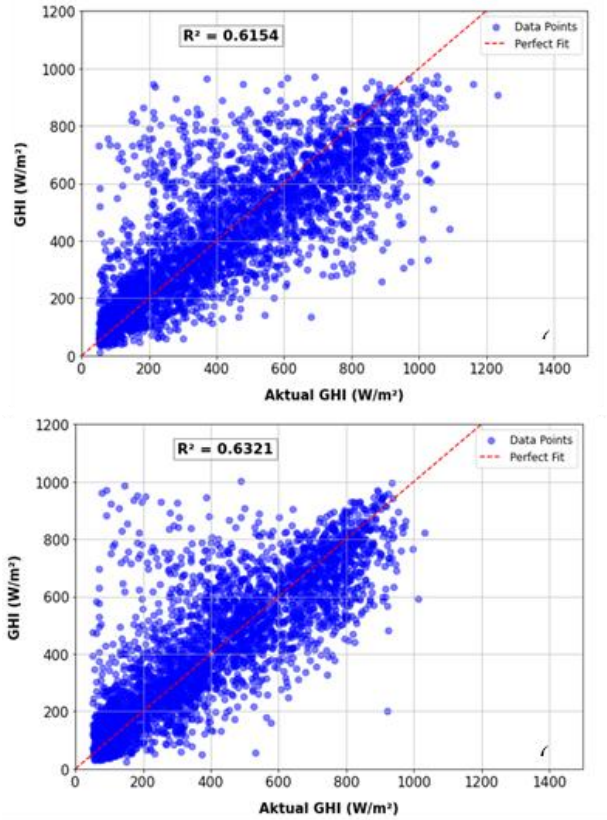

Figure 3-1: Scatterplots of Perez Model.

The scatterplots comparing observed and estimated GHI values for both stations show a relatively strong correlation, with coefficients of determination (R^2) of 0.6154 for IDM1 and 0.6321 for IDM2. As shown in Figure 3-1, these values indicate that more than 60% of the variability in observed GHI can be explained by the model outputs, a significant outcome considering the model's simplicity and the inherent noise in atmospheric conditions. The clustering of data points around the 1:1 fit line further reinforces

the consistency and strength of the model's predictive performance in the Indramayu region.

Overall, the Perez semi-empirical model produced accurate, stable, and low-bias solar irradiance estimates at both Indramayu sites. The region's geographic and atmospheric stability contributed to favorable modeling outcomes, demonstrating that under tropical lowland conditions, the Perez model can effectively capture spatial and temporal patterns in surface-level irradiance. These findings support the use of semi-empirical models for renewable energy assessments in similar environments and confirm the suitability of Indramayu as a reference location for model validation in Indonesia.

3.2 The Spatial Distribution of Solar Irradiance and Topographical Influence

Metric	Station	
	Indramayu 1 (IDM1)	Indramayu 2 (IDM2)
RMSE (W/m^2)	163.52	146.96
rRMSE (%)	37.22	35.36
MBE (W/m^2)	−5.48	12.57
rMBE (%)	−1.24	3.02

During the rainy season (December to February), solar irradiance levels across West Java decrease significantly due to intensified cloud cover, high atmospheric humidity, and increased rainfall. These conditions reduce incoming solar radiation through enhanced scattering and absorption by water vapor and cloud particles. Using the Perez semi-empirical model, spatial estimates of GHI reveal clear patterns that correlate strongly with elevation and regional meteorological behavior. As illustrated in Figure 3-2, GHI values during the rainy season range from approximately 400 to 700 W/m^2.

The highest irradiance levels are observed in the northern lowland regions, particularly in areas such as Indramayu, Karawang, and Subang. These coastal plains, situated at elevations below 500 meters, exhibit more favorable solar conditions due to flatter terrain and relatively stable atmospheric conditions, which limit the vertical development of thick cloud layers. In contrast, central and southern highland regions, including Bandung, Garut, and parts of Sukabumi, display noticeably lower GHI values. These areas

lie within elevation bands of 500–1500 meters and are subject to orographic uplift that promotes persistent cloud formation and increased precipitation. GHI values in these mid- and high-elevation zones are generally limited to 400–500 W/m² during the rainy season, reflecting the impact of mountainous topography on atmospheric clarity.

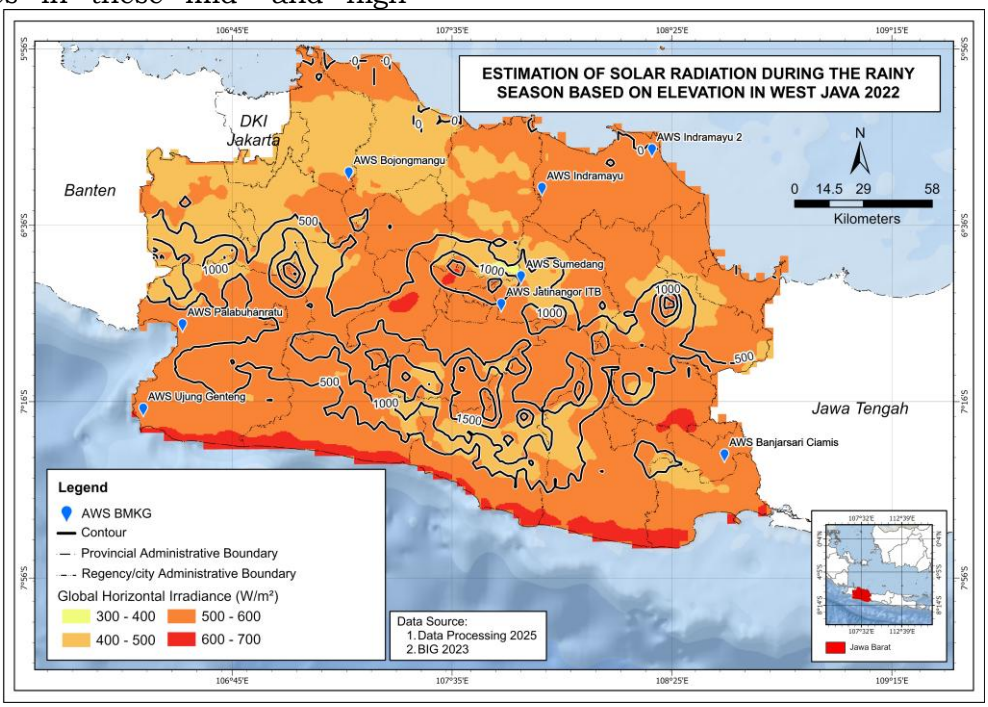

Figure 3-2: Estimated GHI during the rainy season (December–February) in West Java, simulated using the Perez semi-empirical model. Elevation contour lines (500 m, 1000 m, and 1500 m) highlight the relationship between topography and GHI distribution, with higher irradiance observed in lowland areas and reduced values in elevated zones.

The lowest irradiance values are found in elevated mountainous regions above 1000 meters, such as in the surroundings of Mount Ciremai, Mount Gede Pangrango, and other volcanic peaks in southern West Java. These areas experience the strongest orographic effects, resulting in frequent cloud cover and consistently reduced solar exposure. Overall, the Perez model demonstrates a clear relationship between elevation and solar irradiance during the wet season. Lower-elevation areas receive substantially more incoming solar radiation compared to higher terrain, underscoring the importance of considering topography in regional solar energy assessments. This spatial insight is especially valuable for identifying suitable zones for photovoltaic deployment under seasonal variability in tropical environments.

The transition period from the rainy to the dry season in West Java (March to May) is marked by a gradual atmospheric shift—humidity decreases, rainfall lessens, and sky conditions begin to clear. The Perez semi-empirical model responds sensitively to these dynamics, capturing a notable increase in Global Horizontal Irradiance (GHI) compared to the wet season, while still reflecting spatial variability driven by elevation, cloud dynamics, and landform-atmosphere interactions.

As shown in Figure 3-3, much of West Java experiences GHI values in the range of 600–800 W/m², with the highest irradiance occurring in coastal lowland regions. Areas such as Indramayu, Karawang, and parts of Cirebon in the north, as well as Ujung Genteng and Palabuhanratu in the south, exhibit elevated GHI due to declining cloud cover and the absence of orographic uplift that characterizes highland regions. These lowland areas (<500 m above sea level) receive more direct solar radiation because they are less affected by convective cloud formation and exhibit reduced

atmospheric moisture content during this seasonal window.

In contrast, the central mountainous corridor of West Java, which includes Bandung, Garut, and Sumedang, shows a persistent GHI suppression, generally in the range of 400–600 W/m², despite seasonal improvements. Here, terrain-induced cloud retention remains significant. As the air mass cools with altitude, its capacity to hold moisture diminishes, triggering condensation and cloud formation over mid-elevation slopes (500–1000 m). The Perez model reflects this localized atmospheric thickening, capturing the way topographic elevation structures cloud behavior even in transitional seasons.

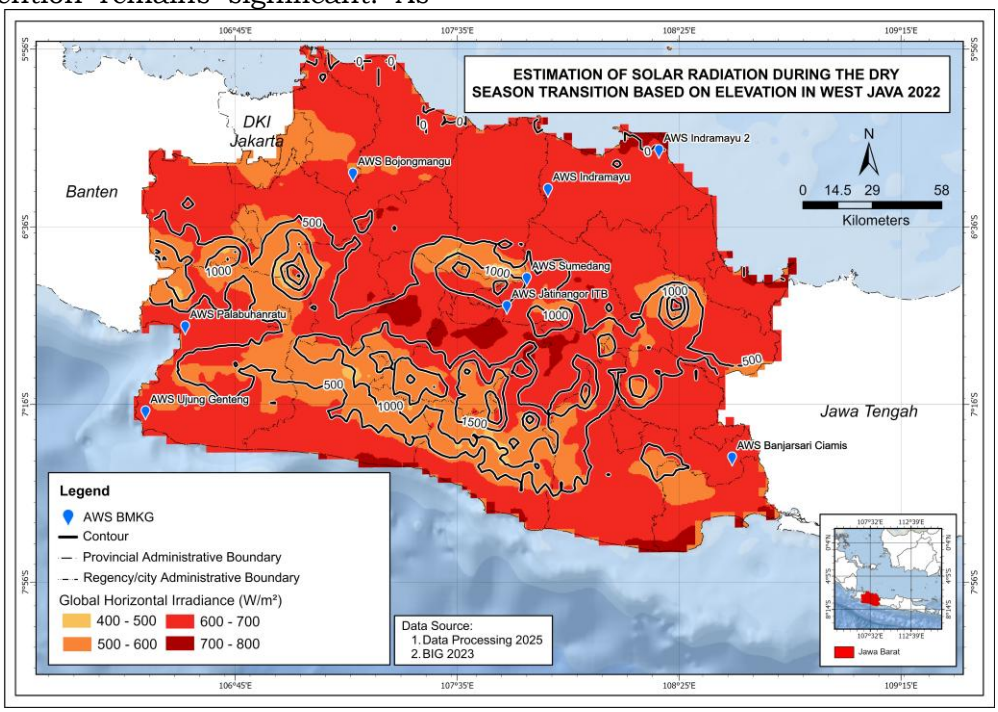

Figure 3-3: Estimated GHI during the transition to the dry season (March–May) in West Java, based on the Perez semi-empirical model. Irradiance values are highest in low-lying coastal areas (<500 m), and decrease with elevation, particularly in mountainous regions above 1000 m, where orographic cloud formation persists despite seasonal improvements.

More pronounced suppression is visible in elevation zones above 1000 meters, such as the volcanic uplands surrounding Mount Gede Pangrango, Mount Ciremai, and the Kendeng mountain chain. These regions exhibit GHI values below 500 W/m². This pattern aligns with physical climatology principles, particularly the orographic enhancement of cloud cover and the atmospheric lapse rate that accelerates condensation processes at higher elevations (Barry 2008). These areas experience higher cloud persistence, resulting in greater diffused radiation and reduced direct irradiance.

Importantly, the Perez model does not merely reflect a seasonal increase in irradiance but also captures the geospatial asymmetry of that increase. Its ability to produce consistently higher values in flat terrain while attenuating irradiance across complex topographies indicates strong model responsiveness to spatial drivers in tropical environments. Unlike simpler empirical approaches that treat seasonal effects homogeneously, the Perez model exhibits fine-scale sensitivity to elevation-linked cloud mechanics, especially during transitional atmospheric phases where variability is high. The spatial pattern of GHI during the March–May period reveals that solar resource availability in West Java is not only a function of seasonal clearing, but also of elevation-driven atmospheric processes. The Perez model provides a geographically coherent and physically plausible estimate of this variability. Its output

underscores the importance of incorporating terrain and transition-season meteorology into solar planning, particularly in regions where solar development may expand beyond coastal corridors into inland and elevated zones.

The dry season in West Java brings a marked shift in solar irradiance conditions, and the Perez semi-empirical model captures this transition with spatial precision. As the region enters its least cloudy months (June–August), radiative transmittance through the atmosphere improves substantially. The model simulates a broad increase in Global Horizontal Irradiance (GHI), signaling a peak in solar energy availability across nearly all elevation zones.

The most prominent GHI values—ranging from 700 to 800 W/m²—are concentrated in the northern coastal plains, particularly in Indramayu, Karawang, and Subang. These regions exhibit the most favorable solar conditions due to a convergence of geographic advantages: low elevation, minimal terrain obstruction, and limited orographic cloud formation. The Perez model recognizes these features, showing how dry-season irradiance maximizes where atmospheric clarity aligns with flat topography.

Topography plays a decisive role in shaping spatial patterns beyond the lowlands. In mid-altitude zones (500–1000 m), such as the Bandung basin and upland valleys of Sumedang and South Cianjur, irradiance remains high but begins to taper. Here, the GHI often ranges between 600 and 700 W/m². The model's output suggests that although dry-season conditions reduce cloud cover overall, these interior regions still experience local circulation effects and temperature-driven cloud formation, particularly in valleys and leeward slopes.

In highland areas exceeding 1000 meters, including volcanic massifs such as Mount Gede Pangrango and Mount Ciremai, the Perez model estimates noticeably lower GHI—generally below 600 W/m². These zones retain more humidity due to persistent orographic uplift, even in the dry season, which limits the amount of direct sunlight reaching the surface. The model's performance here demonstrates its sensitivity to microclimatic variation induced by altitude, reinforcing the elevation–irradiance inverse relationship.

The spatial coherence shown in the Perez model map underscores how elevation is not simply a modifier but a controlling factor. Even under otherwise favorable seasonal conditions, terrain structure continues to regulate the spatial distribution of solar radiation. This has practical implications: regions that might appear viable during general assessments may underperform due to microclimatic suppression tied to altitude. From a development perspective, the model output suggests that lowland and coastal areas are the most reliable zones for dry-season solar harvesting. These locations combine consistently high irradiance with ease of infrastructure access. Meanwhile, upland areas—though improved from the rainy season—require more cautious evaluation due to lingering atmospheric constraints. In conclusion, the Perez model not only quantifies the seasonal solar peak in West Java—it reveals how that peak is distributed, constrained, and geographically patterned. The dry season does not eliminate spatial heterogeneity; rather, it sharpens it. The model's capacity to integrate both clear-sky gains and terrain effects confirms its value in supporting solar energy deployment strategies in tropical monsoon regions.

The September to November period in West Java marks the atmospheric transition from the dry season to the onset of the monsoon. During this time, rainfall frequency begins to rise and convective cloud formation intensifies, especially over elevated terrain. However, sky conditions are not yet as consistently overcast as during peak rainy months, allowing for significant solar irradiance in many parts of the region. The Perez semi-empirical model responds sensitively to this in-between climatological phase, producing Global Horizontal Irradiance (GHI) estimates that reflect both seasonal clarity and localized atmospheric buildup.

As illustrated in Figure 3-4, much of northern and central West Java maintains relatively high GHI levels during this season. Areas such as

Indramayu, Subang, and parts of Sumedang and Jatinangor consistently show GHI values in the 600–700 W/m² range, with some zones reaching or exceeding 700 W/m². These regions are situated on low-elevation plains where cloud formation is less persistent, and the atmosphere remains more transparent during early-stage moisture accumulation. The Perez model captures this well, producing a stable and spatially coherent pattern that emphasizes the lingering radiative advantage in flat, coastal, and basin regions.

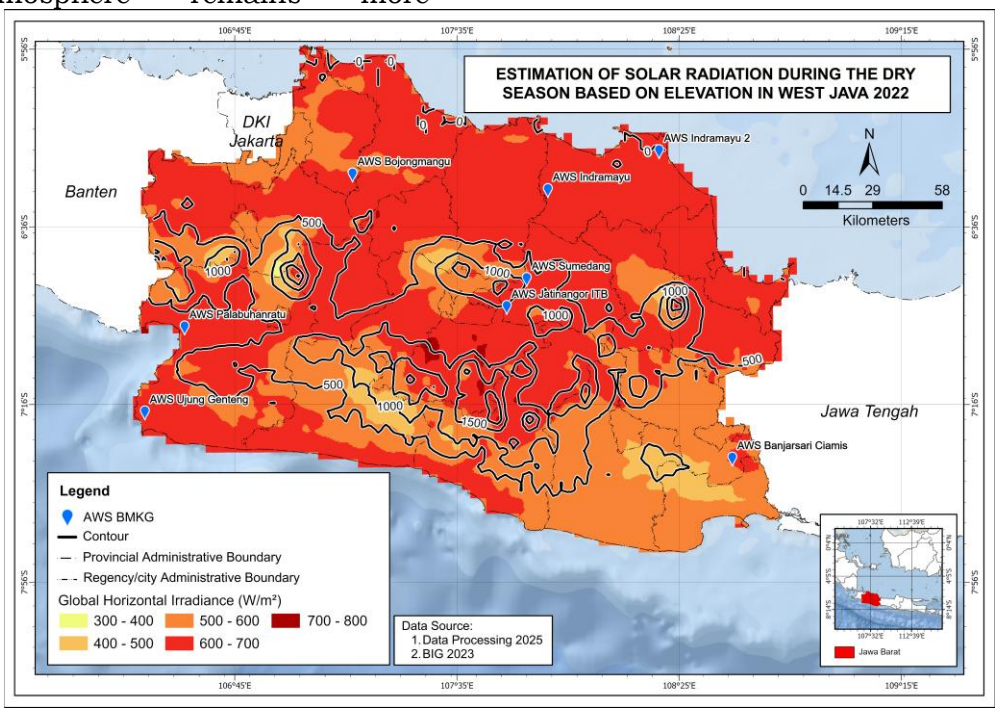

Figure 3-4: Estimated Global Horizontal Irradiance (GHI) during the dry season (June–August) across West Java using the Perez semi-empirical model. Areas in red (GHI 700–800 W/m²) are concentrated in northern coastal lowlands, while irradiance decreases with elevation, particularly in mountainous zones above 1000 m.

Moving into mid-elevation areas (500–1000 m), such as the Bandung Basin, North Garut, and much of Purwakarta, irradiance begins to taper. GHI estimates in these regions typically fall into the 500–600 W/m² range, reflecting a transition in atmospheric behavior. Here, the increasing moisture content and afternoon convective cloud development act to scatter incoming radiation and reduce direct solar flux to the surface. The model's gradation in these zones demonstrates its responsiveness to daily atmospheric instability common during monsoon onset.

In contrast, the highland regions above 1000 meters—such as the volcanic ranges around Mount Gede, Mount Ciremai, and the southern plateau near Garut and Ciamis—exhibit the lowest GHI estimates during this period. These zones are frequently enveloped in dense orographic clouds and experience higher humidity, which amplifies scattering and diffusive losses. The Perez model assigns these areas GHI values generally below 500 W/m², aligning with observed climatological tendencies in tropical highlands during seasonal transitions.

This spatial pattern reinforces the inverse relationship between elevation and irradiance across seasons in West Java, and more importantly, demonstrates the model's capability to reflect microclimatic conditions rather than just regional averages. What is notable during this transition phase is the increased spatial contrast between lowland and upland areas. While in the dry season even highlands benefit from improved sky clarity, the transition period reintroduces vertical stratification

in cloud thickness, which the Perez model captures with appropriate suppression of GHI in mountainous zones.

From a spatial planning perspective, the model's output during this season suggests that northern lowlands and inland depressions retain their potential for solar energy harvesting despite rising humidity. This highlights the model's utility in supporting infrastructure design that accounts for seasonal intermittency. The ability of the Perez model to simulate these patterns—based on cloud index, clear-sky baselines, and topographic factors—offers a reliable framework for tropical solar energy forecasting under transitional atmospheric dynamics. The seasonal dynamics of solar irradiance in West Java, as simulated by the Perez model, reveal consistent spatial structuring driven largely by elevation, atmospheric moisture, and cloud development. Across all four seasonal phases, lowland regions—particularly the northern coastal plain encompassing Indramayu, Subang, and Karawang—consistently exhibit the highest GHI, with values often ranging between 600–800 W/m² during the dry and transitional months. These areas benefit from minimal topographic interference, reduced orographic uplift, and more stable atmospheric clarity throughout the year, making them highly favorable for solar energy harvesting. By contrast, upland and mountainous zones such as the Bandung highlands, Garut, and Mount Gede Pangrango repeatedly show suppressed irradiance, particularly during the rainy and transition-to-rainy periods. These patterns underscore a strong and persistent inverse correlation between elevation and GHI, shaped by microclimatic cloud behavior and terrain-induced humidity retention.

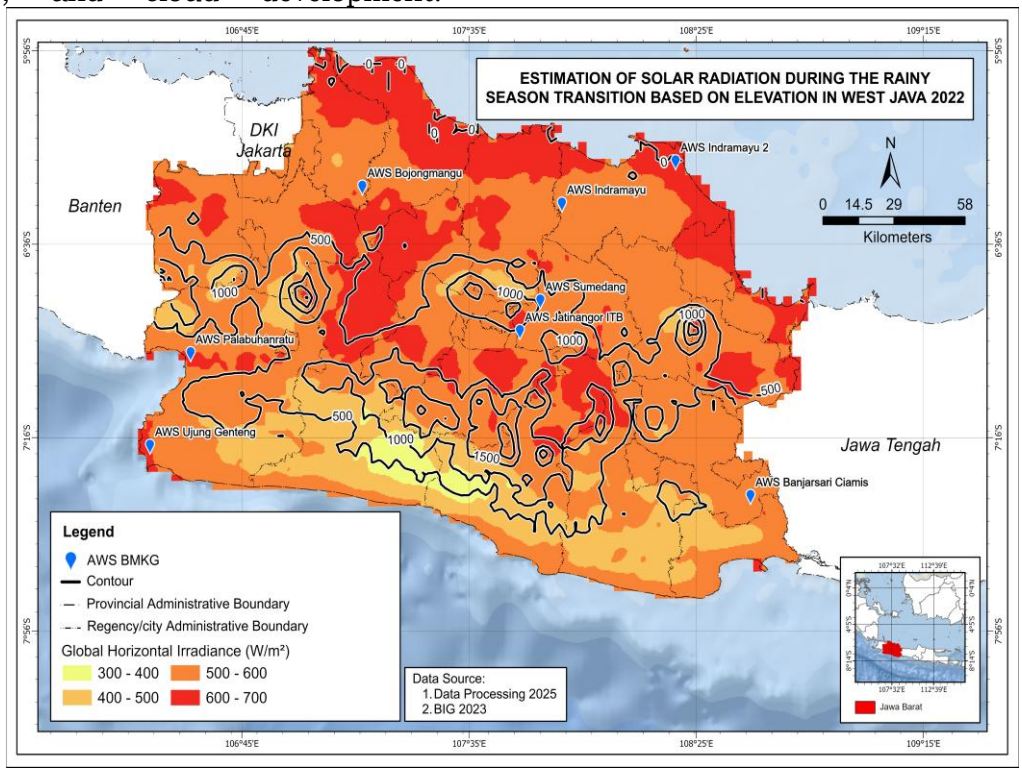

Figure 3-5: Estimated Global Horizontal Irradiance (GHI) during the September–November transition to the rainy season in West Java, modeled using the Perez semi-empirical approach. GHI values remain high in northern lowlands and inland basins (600–700 W/m²), while mountainous zones above 1000 m show lower irradiance due to increased cloud formation and atmospheric moisture.

However, it must be noted that the accuracy validation in this study was limited to two BMKG stations located in northern coastal lowlands. No ground-based observations were available for mid- or high-elevation zones, which are central to the spatial analysis presented. As such, while modeled patterns suggest plausible elevation-linked attenuation, these findings are not empirically verified in complex terrain. Future studies should incorporate additional validation datasets from upland and mountainous regions to enhance confidence in model performance across varied topographic zones.

While seasonal changes do affect the magnitude of GHI—peaking during the dry season and declining during the monsoon onset—the spatial logic remains remarkably stable. Low-lying regions always outperform highlands in terms of irradiance, and mid-elevation zones consistently display transitional behavior. Notably, the transition seasons (March–May and September–November) demonstrate heightened spatial contrast, with clearer skies in lowlands coexisting with intensified cloud formation in highlands. This reinforces the importance of terrain-aware forecasting in tropical regions. The Perez model has proven capable of capturing these seasonal-spatial interactions, balancing atmospheric inputs and surface factors to produce coherent and reliable irradiance estimates. Its performance affirms its suitability for operational solar energy planning across climatically complex tropical geographies like West Java.

Despite the promising performance of the Perez semi-empirical model in simulating seasonal and spatial variations of GHI across West Java, this study acknowledges several limitations. First, the model's accuracy was validated using observational data from only two BMKG stations, both situated in northern coastal lowlands. This leaves mid- and high-elevation zones—central to the spatial analysis—without ground-truth validation, potentially underestimating local performance deviations in more complex terrain. Second, no comparative benchmarking was conducted against alternative modeling approaches such as empirical regressions, physical radiative transfer models, or machine learning frameworks. Without such comparisons, the relative strengths and weaknesses of the Perez model remain unexplored in the context of West Java's climatic and topographic diversity. Additionally, the use of hourly temporal resolution may influence the model's applicability for photovoltaic system planning, especially in cases requiring sub-hourly granularity.

Finally, the representativeness and spatial coverage of key input datasets, such as AERONET and GK2A, were not explicitly evaluated, leaving room for further analysis of potential satellite viewing geometry bias, cloud contamination, and surface heterogeneity. Future work should address these gaps by incorporating higher-altitude validation sites, expanding temporal resolution analysis, and testing alternative models under identical atmospheric inputs.

4 CONCLUSION

This study presents a comprehensive spatial and temporal assessment of solar irradiance in West Java using the Perez semi-empirical model. Focusing on four seasonal phases—rainy season, transition to dry, dry season, and transition to rainy—the analysis reveals clear seasonal variability and strong spatial coherence in the distribution of Global Horizontal Irradiance (GHI). The Perez model demonstrates its suitability for modeling solar radiation in tropical regions, successfully integrating topographic and atmospheric dynamics to estimate irradiance across diverse elevation zones. The study confirms that solar energy potential in West Java is both seasonally dynamic and geographically structured, offering key insights for renewable energy planning.

In terms of accuracy, the Perez model produces reliable and stable estimates when validated against observed GHI data, particularly in lowland regions such as Indramayu. The model demonstrates low RMSE and bias values at selected validation stations, and it maintains relative error levels within acceptable thresholds for

operational use. Its ability to perform well under conditions of limited atmospheric data makes it especially appropriate for tropical contexts like Indonesia, where continuous high-resolution atmospheric datasets remain sparse. The validation results confirm that the Perez model not only captures general irradiance trends but is also responsive to local climatological variability.

The spatial distribution analysis reveals a persistent pattern across all seasons: lower elevation areas—especially coastal and basin regions—consistently receive higher solar radiation compared to the mountainous central and southern zones of West Java. This gradient is driven by topography-induced cloud formation, atmospheric moisture concentration, and orographic effects. Seasonal improvements in sky clarity, particularly during the dry and transition-to-dry seasons, amplify irradiance in most areas, but highland regions remain limited due to persistent cloud presence. The spatial logic modeled by Perez affirms the importance of integrating terrain, seasonality, and cloud dynamics into solar energy assessments in humid tropical regions.

Looking forward, future research should explore integrating the Perez model with more frequent satellite-based cloud dynamics and higher-resolution DEMs to improve local accuracy, particularly in complex terrains. Incorporating real-time atmospheric corrections and expanding validation networks across elevation bands would enhance the robustness of solar forecasting in Indonesia. Overall, this study affirms the value of semi-empirical modeling in capturing spatiotemporal solar variability in tropical landscapes and provides a solid foundation for advancing solar energy planning in West Java and other geographically complex regions.

ACKNOWLEDGEMENTS

This study was financially supported by grants from HIBAH PUTI Q1 2024–2025 of DRPM UI University of Indonesia (NKB-420/UN2.RST/HKP.05.00/2024).

REFERENCES

Albadi M, Al-Badi A, (2021), Solar photovoltaic power intermittency and implications on power systems. Cambridge Scholars Publishing.

Alpandino, (2011), Solar radiation in tropical mountain ecosystems. Available via DIALOG. https://alpandino.org/en/course/02/02b.htm. Accessed 23 May 2025.

Barry RG, (2008), Mountain weather and climate. Cambridge University Press.

BNPB, (2020), Dokumen Rencana Penanggulangan Bencana Provinsi Jawa Barat. Jakarta: BNPB.

BNPB, (2022), Rencana Penanggulangan Bencana Provinsi Jawa Barat 2022–2026. Jakarta: BNPB.

BPS, (2024), Provinsi Jawa Barat dalam angka 2024. Jawa Barat: Badan Pusat Statistik Provinsi Jawa Barat.

Beck HE, McVicar TR, Vergopolan N, et al., (2023), High-resolution (1 km) Köppen-Geiger maps for 1901–2099 based on constrained CMIP6 projections. Scientific Data, 10:724. doi:10.1038/s41597-023-02549-6

Beyer HG, Costanzo C, Heinemann D, (1996), Modifications of the Heliosat procedure for irradiance estimates from satellite images. Solar Energy, 56(3):207–212.

Cai Q, Qing J, Zhong C, et al., (2024), Temporal and spatial heterogeneity analysis of wind and solar power complementarity and source-load matching characteristics in China. Energy Conversion and Management, 315:118770. doi:10.1016/j.enconman.2024.118770

Chen S, Liang Z, Guo S, & Li M, (2022), Estimation of high-resolution solar irradiance data using optimized semi-empirical satellite method and GOES-16 imagery. Solar Energy, 241:404–415. doi:10.1016/j.solener.2022.06.013

EIU, (2023), Energy Outlook 2024: Surging demand defies wars and high prices. Economist Intelligence Unit.

El-Amarty N, Marzouq M, El Fadili H, et al, (2023), A comprehensive review of solar irradiation estimation and forecasting using artificial neural networks: Data, models and trends. Environmental Science and Pollution Research, 30:5407–5439. doi:10.1007/s11356-022-24240-w

ESDM, (2019), Statistik Energi Sumber Daya Mineral 2019. Jakarta: Direktorat Jenderal Minyak dan Gas Bumi.

ESDM, (2021), Menteri ESDM: Cadangan Minyak Indonesia Tersedia untuk 9,5 Tahun dan Cadangan Gas 19,9 Tahun. Available via DIALOG. https://www.esdm.go.id/id/media-center/arsip-berita/menteri-esdm-cadangan-minyak-indonesia-tersedia-untuk-95-tahun-dan-cadangan-gas-199-tahun. Accessed 24 May 2025.

ESDM, (2023), Handbook of Energy & Economic Statistics of Indonesia 2023. ESDM.

ESDM, (2024), Konferensi Pers Capaian 2023, Konsumsi Per Kapita Lebihi Target. Available via DIALOG. https://www.esdm.go.id/id/media-center/arsip-berita/menteri-esdm-cadangan-minyak-indonesia-tersedia-untuk-95-tahun-dan-cadangan-gas-199-tahun. Accessed 17 October 2024.

Escobar RA, Ortega A, Cortés C, et al., (2014), Solar energy resource assessment in Chile: Satellite estimation and ground station measurement. Energy Procedia, 57:1257–1265. doi:10.1016/j.egypro.2014.10.115

Gürel AE, Ağbulut Ü, Bakır H, Ergün A, Yıldız G, (2023), A state of art review on estimation of solar radiation with various models. Heliyon, 9(2). doi:10.1016/j.heliyon.2023.e13167

Halabi LM, Mekhilef S, Hossain M, (2018), Performance evaluation of hybrid adaptive neuro-fuzzy inference system models for predicting monthly global solar radiation. Applied Energy, 213:247–261. doi:10.1016/j.apenergy.2018.01.035

Hammer A, Heinemann D, Hoyer C, et al., (2003), Solar energy assessment using remote sensing technologies. Remote Sensing of Environment, 86(3):423–432. doi:10.1016/S0034-4257(03)00083-X

IESR, (2021), Indonesia Energy Transition Outlook 2021. Institute for Essential Services Reform.

IEA, (2023), World Energy Outlook 2023. International Energy Agency.

Kleissl J, (2013), Solar energy forecasting and resource assessment. Elsevier. doi:10.1016/C2011-0-07022-9

Maka AO, Ghalut T, Elsaye E, (2024), The pathway towards decarbonisation and net-zero emissions by 2050: The role of solar energy technology. Green Technologies and Sustainability 2(3). doi:10.1016/j.grets.2024.100107

Napoli A, Crespi A, Ragone F, et al., (2019), Variability of orographic enhancement of precipitation in the Alpine region. Scientific Reports, 9(1):1–9. doi:10.1038/s41598-019-49974-5

Perez R, Ineichen P, Moore K, et al., (2002), A new operational model for satellite-derived irradiances: Description and validation. Solar Energy, 73(5):307–317.

PLN, (2024), Statistik PLN 2023. Jakarta: PT PLN (Persero).

Remund J, Wald L, Lefevre M, Ranchin T, Page J, (2003). Worldwide Linke turbidity information. In ISES Solar World Congress 2003. Göteborg, Sweden, June 2003.

Sarr A, Kebe CM, Gueye M, Ndiaye A, (2021), Impact of temporal and spatial variability of solar resource on technical sizing of isolated solar installations in Senegal using satellite data. Energy Reports, 7(5):753–766. doi:10.1016/j.egyr.2021.07.064

Scarpa F, Bianco V, & Tagliafico LA, (2018), A clear sky physical based solar radiation decomposition model. Thermal Science and Engineering Progress, 6:323–329. doi:10.1016/j.tsep.2017.11.004

Tscholl S, Tasser E, Tappeiner U, Egarter Vigl L, (2022), Coupling solar radiation and cloud cover data for enhanced temperature predictions over topographically

complex mountain terrain. International Journal of Climatology, 42(11):4684–4699. doi:10.1002/joc.7497

Worldometer, (2024), How many countries are there in the world?. Available via DIALOG. https://www.worldometers.info/geography/how-many-countries-are-there-in-the-world/. Accessed 17 October 2024.

Zhang C, Guo Y, He Z, et al., (2022), Analysis of influence mechanism of spatial distribution of incoming solar radiation based on DEM. Earth Science Informatics, 15:635–648. doi:10.1007/s12145-021-00740-0

Zhang X, Xia P, Peng F, et al., (2024), Multiple spatial-temporal scales assessment of solar and wind resources potential integrating geospatial-technology-correlation indicators: A case study of Hunan Province. Energy, 304, vol 132036. doi:10.1016/j.energy.2024.132036